# Temperature dependence of the intrinsic remanent magnetization and anisotropy energy in the spin glass Cu-Mn

Dojun Youm and S. Schultz

*University of California, San Diego, La Jolla, California 92093*

We have measured the temperature and dc magnetic field dependence of the parallel and perpendicular ac susceptibilities of the spin glass Cu—5 at. % Mn at a frequency of 30 Hz. The temperature range is above and below $T_g^0$, the spin-glass transition temperature in zero field. From an analysis of these ac data, in conjunction with that for the dc magnetization, we are able to determine the $T$ and $H$ dependence of a quantity we identify as the intrinsic magnetic remanence, $M_{IR}$. The advantage of studying $M_{IR}$ is that it is determined at each measurement frequency by time-independent measurements. We find $M_{IR}$ obeys the simple power-law relation $M_{IR} \propto (1 - T/T_g^0)^{1/2}$ for all $T < T_g^0$. We also have determined the $T$ and $H$ dependence of the total anisotropy constant and find that it obeys a linear relation which extrapolates to zero near $T_g^0$, in contrast to a much higher temperature found from ESR measurements at 9 GHz. We suggest that a systematic study of $M_{IR}$ over an extended frequency range should provide a valuable set of data for gaining insight into the complex time dependence of spin-glass variables.

## I. INTRODUCTION

At present there is still a considerable lack of knowledge of the experimentally determinable time (or frequency) dependence of the spin-glass state, and a corresponding lack of understanding of the appropriate theoretical description as well.[1] In this paper we present measurements of the ac susceptibility (both parallel and perpendicular to the dc field) for a frequency of 30 Hz over an extensive range of dc field and for temperatures above and below $T_g^0$, the spin-glass transition temperature in zero field.[2] We also measure the dc magnetization as a function of dc field and temperature. From an analysis of these data we are able to determine the temperature dependence of the intrinsic (magnetic) remanence $M_{IR}$ (defined explicitly below) and the anisotropy constant $K$ (both) corresponding to the frequency of measurement, i.e., 30 Hz. We find that the intrinsic magnetic remanence is well described by a power law, $M_{IR} \propto (1 - T/T_g^0)^{1/2}$, and that the anisotropy energy appears to go to zero at $T_g^0$, in distinct contrast to the behavior found at very high (e.g., ESR) frequencies.[3]

The advantage of our approach, based on the determination and subsequent utilization of the *intrinsic* magnetic remanence is that we are able to make *time-dependent* measurements (at any given frequency) and thereby obtain meaningful results much closer to $T_g$ than has hitherto been possible. Although we only report a complete set of data at one frequency (30 Hz), we have made preliminary measurements at frequencies as diverse as 700 and $10^{-3}$ Hz, and believe that our approach may be readily extended to a larger frequency range. We suggest that the appropriate theoretical analysis of such a set of data may be most valuable in understanding the spectrum of relaxation times underlying the dynamics of the spin-glass state.

We will present data for the temperature and dc field dependence of both the parallel and perpendicular ac susceptibility and dc magnetization for several Cu-Mn spin-glass alloys. Our analysis of these data is based on the ansatz that the total magnetization may always be represented as the sum of a reversible and irreversible component in a manner discussed by Duynenveldt and Mulder.[4] Before we can present the data we first introduce our definitions and operational procedures in some detail.

A given ac susceptibility is defined as the differential magnetization at the frequency, and in the direction of, the corresponding applied ac magnetic field. When the ac field, $\mathbf{h}(\omega)$, is parallel to the applied dc magnetic field, $\mathbf{H}$, we measure $\mathcal{X}_{||}$, the parallel susceptibility. When $\mathbf{h}$ is perpenidcular to $\mathbf{H}$, we measure $\mathcal{X}_{\perp}$, the perpendicular susceptibility. We also measure the dc magnetization, $M_{dc}$, for a given constant $H$, as a function of temperature, and their ratio will be referred to as $\mathcal{X}_{dc}$.

Examples of typical data are presented in Fig. 1. Curve (a) represents $\mathcal{X}_{||}$ as measured for zero applied dc field, and exhibits the well-known peak[2] at the zero-field spin-glass transition temperature, $T_g^0$. Curves (b), (c), and (d) are all for an applied dc field $H = 1.2$ kG, and represent respectively, $\mathcal{X}_{||}$, $\mathcal{X}_{\perp}$, and $\mathcal{X}_{dc}$.

We may note the extensive suppression of $\mathcal{X}_{||}$ by the applied dc field, and that there is a $T$-independent region which abruptly changes slope at a temperature which is well below $T_g^0$. We have suggested that this temperature represents $T_g(H)$, i.e., the spin-glass transition temperature in finite field.[5] In the paper of Ref. 5 we identify the transition as occurring at the divergence of a new rotational correlation length associated with the internal field, and have developed a theoretical model and interpretation which quite satisfactorily predicts $T_g(H)$ from an analysis of the $\mathcal{X}_{||}(H,T)$ and $M_{dc}$ data.

We now seek to establish several interesting relations among the various susceptibilities. However, we must distinguish the temperature region above and below $T_g(H)$
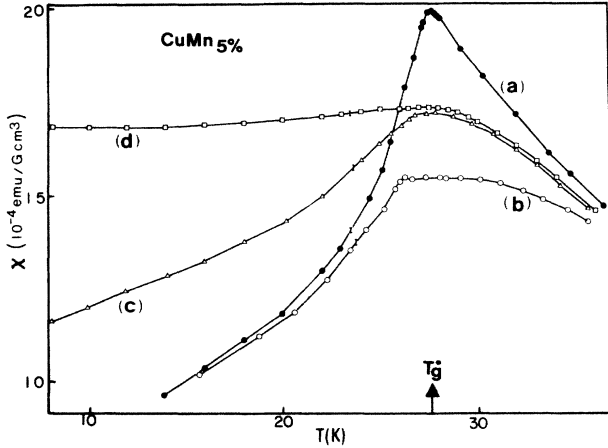
FIG. 1. Typical data of the three susceptibilities measured in this study as a function of temperature. (a) The parallel ac susceptibility, $\chi_{||}$, in zero applied field. (b), (c), and (d) are all measured in a field of 1.2 kG and represent respectively, $\chi_{||}$, $\chi_{\perp}$, and $\chi_{dc}$. (These $\chi$ and their relationships are defined explicitly in the text.)



$$\frac{m_{rev}}{M_{rev}} = \frac{h}{H_{dc}} \qquad \frac{m_{IR}}{M_{IR}} \simeq \frac{h - H_a}{H_{dc}}$$
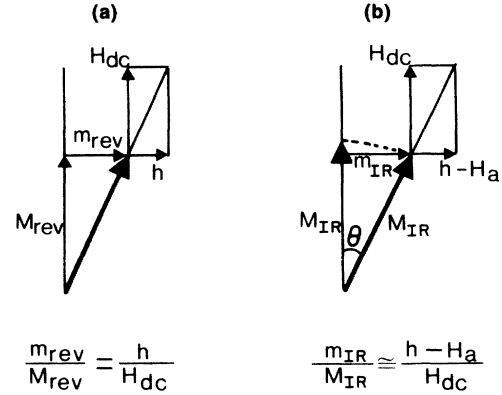
FIG. 2. The geometric relations for the magnetization and magnetic field corresponding to $\chi_{\perp}$. (a) The relationship of the ac and dc magnetization components, $m_{rev}$ and $M_{rev}$, corresponding to the field values when the temperature is above $T_g$. (b) The relationship of the irreversible components of the magnetization, $m_{IR}$ and $M_{IR}$, to the ac field, $h$, the applied field, $H_{dc}$, and the anisotropy field, $H_a$, when the temperature is below $T_g$.

separately.

**Case a:** $T > T_g(H)$. Above the spin-glass transition temperature $T_g(H)$, the total magnetization $\mathbf{M}_T$ is regarded as being completely reversible for the frequency of the ac measurements. [Hence, $\mathbf{M}_T$ is always parallel to the instantaneous total applied field, $\mathbf{H}_T = \mathbf{H} + \mathbf{h}(\omega)$.] Since $\chi_{||} = dM_T/dh = dM_{dc}/dH$, if one measures $\chi_{||}$ as a function of $H$ we may determine $M_{dc}(H)$ either by a direct measurement in the field $H$, or by evaluation of the integral of $\chi_{||}$ with respect to $H$. We shall refer to that part of the magnetization that can be so evaluated as $M_{rev}(H) = \int_0^H \chi_{||}(\omega) dH$, i.e., the reversible magnetization corresponding to the applied dc field, $H$. (If we divide $M_{rev}$ by $H$ we obtain $\chi_{rev}$.)

We now establish the relationship of $\chi_{\perp}$ to the quantities just discussed. In Fig. 2(a) we illustrate how, when $\mathbf{h}(\omega)$ is applied perpendicular to $\mathbf{H}$, there is a corresponding perpendicular component of $\mathbf{M}_T$ labeled as $m_{rev}$. As can be seen,

$$\chi_{\perp} = m_{rev}/h = M_{rev}/H = (1/H) \int_0^H \chi_{||} dH .$$

Thus, above $T_g(H)$ we see that $\chi_{\perp} = \chi_{rev}$ and should equal $\chi_{dc}$, which imposes an important self-consistency test of the data. (As can be seen in Fig. 5, our data agree with this relation to within the experimental uncertainties.)

**Case b:** $T < T_g(H)$. Below $T_g(H)$ it is observed that there is an irreversible component to the magnetization, and an associated anisotropy energy. At temperatures below $\approx T_g/2$, the irreversible magnetization may be readily demonstrated by simply turning off the applied dc (cooling) field, and measuring the thermal remanent magnetization (TRM). Alternatively, the sample may be cooled in weak fields to $T \ll T_g$, subjected briefly to a larger field ($H \approx 10$ Kg), turn off the field and an appreciable isothermal remanent magnetization (IRM) will result. Such TRM and IRM studies have also revealed that the remanence decays[6] or grows[7] with a logarithmic time

dependence. The characteristic time scale of the decay, however, is a function of temperature, and the combination of a smaller remanence and the faster decay rate eventually prevent an accurate determination as one approaches $T_g$.

We adopt an alternate approach to the study of the remanence in spin glasses which circumvents the difficulties just described. We define an intrinsic remanence, $M_{IR}(\omega)$ which may be readily determined at fixed frequency and arbitrary $T$ and $H$ by a measurement of the $M_{dc}$ and the field dependence of $\chi_{||}$. Here $M_{dc}$ is the field-cooled magnetization. Because the cooling field, $H$, is always fixed, $M_{dc}$ is independent of time. Once $M_{IR}$ is known, one can then interpret the $\chi_{\perp}$ data to determine the anisotropy constant as a function of $T$ and $H$.

We assume that the dc magnetization at any $T$ and $H$ may be represented as the sum of a reversible and an intrinsic irreversible magnetization component. The key concept is that if we identify the reversible component, $M_{rev}(\omega)$, as being determined with respect to a particular time scale (or frequency), then the intrinsic irreversible component $M_{IR}(\omega)$ is similarly so associated. Thus, we may write (for all $T$ and $H$) and field $\omega$,

$$\mathbf{M}_{dc}(H,T) = \mathbf{M}_{rev}(\omega, H, T) + \mathbf{M}_{IR}(\omega, H, T) ,$$

and using $M_{rev} = \int_0^H \chi_{||} dH$ we have

$$\mathbf{M}_{IR}(\omega, H, T) = M_{dc}(\omega, H, T) - \int_0^H \chi_{||}(\omega, H, T) dH . \qquad (1)$$

If we divide all quantities in Eq. (1) by $H$ we obtain the intrinsic irreversible susceptibility $\chi_{IR}(\omega, H, T)$. We may alternatively think of this irreversible magnetization component as an intrinsic magnetic remanence, since it represents that component of the total magnetization that does not respond in time, at least over the scale set by the measuring frequency. Thus, if the dc field were turned off in a time comparable to the period of $\omega$, one should find a remanence, $M_r$, very nearly equal to $M_{IR}$.

Returning to Fig. 2, we may now interpret the measured $\chi_\perp$ below $T_g(H)$ in a manner analogous to that proposed by Hippert and Alloul.[8] The application of an **h** perpendicular to the **H** will result in a reversible component of the magnetization, $\mathbf{m}_{rev}$, as in the case for $T > T_g$, with $m_{rev}/h = (1/H)\int_0^H \chi_{\parallel} dH$. In addition there will be another component, $\mathbf{m}_{IR}$, representing the rotation of $\mathbf{M}_{IR}$. The magnitude of $m_{IR}$ will be determined by a balance of the driving and restoring torques associated with the Zeeman and anisotropy energy, respectively. Since we are always dealing with small angles of rotation, $\theta$, we may take our anisotropy energy as[9] $E_a = k\theta^2/2$ and define the corresponding anisotropy field $H_a = K\theta/M_{IR}$. As illustrated in Fig. 2(b) we see $m_{IR}/M_{IR} \cong h - H_a/H$, but as $H_a \cong K\theta/M_{IR} \cong Km_{IR}/M_{IR}^2$ we solve for $m_{IR}/h$ and find,

$$m_{IR}/h = M_{IR}^2/(M_{IR}H + K) \ .$$

Thus the total $\chi_\perp$ is

$$\chi_\perp = (1/H)\int_0^H \chi_{\parallel} dH + M_{IR}^2/(HM_{IR} + K) \ . \tag{2}$$

[Now we may note that Eq. (2) holds for all $T$, since above $T_g(H), M_{IR}$ is zero.]

In Sec. III we will present our data for $\chi_{\parallel}(H,T)$, which, in conjunction with $\chi_{dc}$ enables us to obtain $\chi_{IR}(H,T)$ or equivalently $M_{IR}$. Knowing $M_{IR}$ and given our $\chi_\perp$ data we can invert Eq. (2) and obtain $K(H,T)$. We interpret our results of the temperature dependence of $M_{IR}$ and $K$ in Sec. IV.

## II. EXPERIMENTAL TECHNIQUES

The samples were prepared by first forming an arc-melted button which was annealed under Ar at 700 °C for one day. The buttons were then rolled to foils 0.002 $\mu$m thick. Samples $0.4 \times 6$ cm$^2$ were vacuum annealed at 800 °C for one hour, and then air cooled. The ac susceptibility measurements were obtained primarily at 30 Hz in two types of apparatus. The sample was always moved between a pair of astatically wound coils which were located in the appropriate ac and dc magnetic fields. The dc field was varied from 0 to 7 kG, the ac field was at 30 Hz and typically $\simeq 2$ G. In one apparatus the output signal from the coils was detected utilizing field-effect transitor (FET) electronics in a circuit incorporating electronic balancing signals as discussed below. In the other, the signal was measured utilizing superconducting coils and an associated superconducting quantum-interference device (SQUID) detector. The measurements of the dc magnetization were performed using a commercial SQUID magnetometer.[10]

The block diagram of the FET based instrument is shown in Fig. 3. An audio oscillator (1) provided the drive current to the primary coil (2). The oscillator output is also connected to a variable gain amplifier (5) and phase shifter (6). The output from the astatically wound pair of coils (3) is initially amplified (4) using a preamplifier, and then summed with the output of the phase shifter. The output of the summing circuit (7) is additionally filtered (8) and then detected by a lock-in amplifier (9) refer-
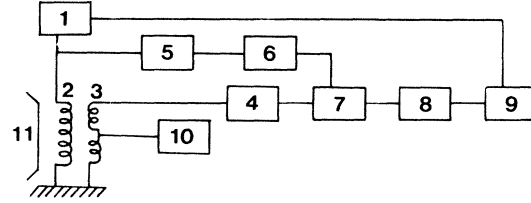


FIG. 3. Block diagram of the ac susceptibility apparatus utilizing FET electronics. (1) the audio frequency oscillator, (2) primary coil for ac field, (3) pair of astatically wound signal coils, (4) FET preamplifier, (5) variable gain amplifier, (6) phase shifter, (7) summing circuit, (8) narrow-band filter, (9) lock-in amplifier, (10) DVM, (11) dc magnet. The sample is moved between the two signal coils as described in the text and illustrated in Fig. 4.
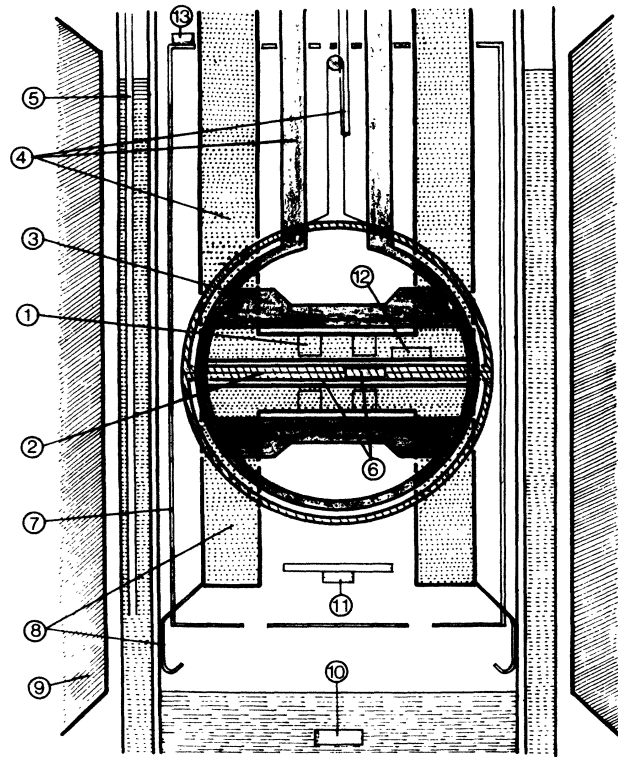


FIG. 4. Detailed scale drawings of the coils and sample arrangement. (1) the astatically wound pickup coils, (2) fine string used to push/pull the sample between the two coils of (1), (3) the primary ac coil, coaxial to (1), (4) various parts of the support system to hold coils firmly in helium Dewar, (5) a fine gas tube in liquid nitrogen jacket through which gas is blown to reduce bubbling, (6) sample holder containing rolled foil sample which slides in plastic tube, (7) temperature shield, (8) massive plastic holder with spring fingers to reduce vibration in helium Dewar, (9) external dc magnetic field, Varian rotatable magnet with 4-in. gap, (10) heater in liquid helium to produce cooling vapor, (11) heater on thermal shield to regulate temperature, (12) cryogenic thermometer, (13) additional heater to maintain shield at desired uniform temperature.
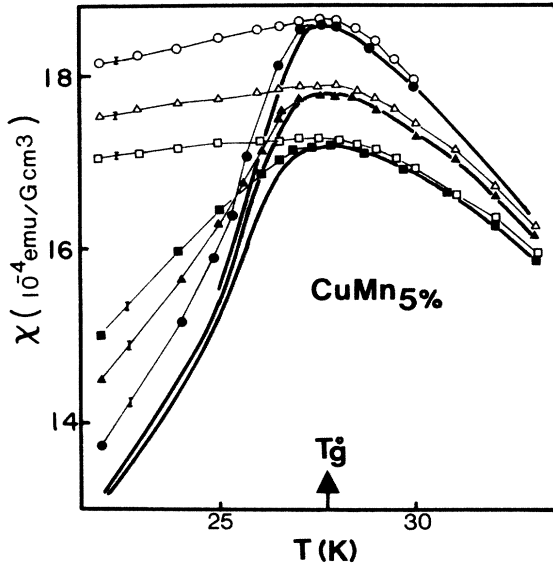
FIG. 5. A comparison of the quantities $\chi_{dc}$ (open symbols) and $\chi_{\perp}$ (closed symbols) for the three dc field values indicated in the figure, as a function of temperature for a Cu–5 at. % Mn spin-glass sample. (The data points are connected by fine lines as a guide to the eye.) The circles, triangles, squares represent 0.4, 0.8, and 1.2 kG dc field, respectively. The heavy lines are values obtained by evaluating $\chi_{rev}=(1/H)\int_0^H \chi_{\parallel}dH$. We see that the three quantities $\chi_{dc}$, $\chi_{\perp}$, and $\chi_{rev}$ all agree within the experimental error for temperatures above $T_g$.
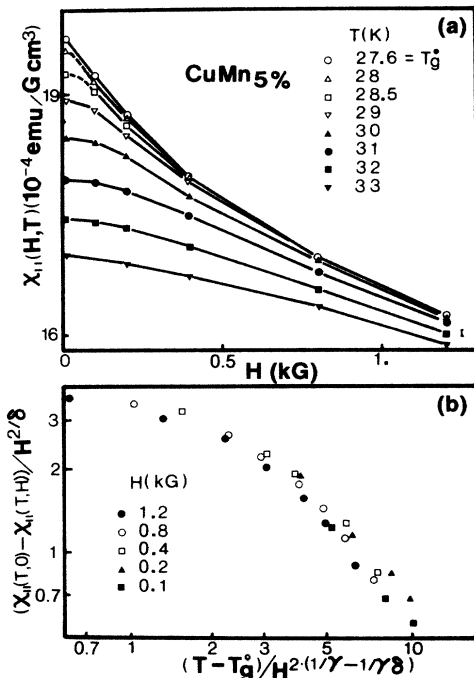


FIG. 6. (a) Values of $\chi_{\parallel}$ as a function of applied dc magnetic field for several values of temperature, all above $T_g^0$. The integral $\int_0^H \chi_{\parallel}dH$ as drawn in Fig. 5 (solid lines) for example, were obtained by integrating these curves. (b) The data of Fig. 6(a) plotted as shown by the labeled axis. We find the data well represented by the scaling (Ref. 11) with $\delta=3+0.8$ and $\gamma=1.85+0.5$.
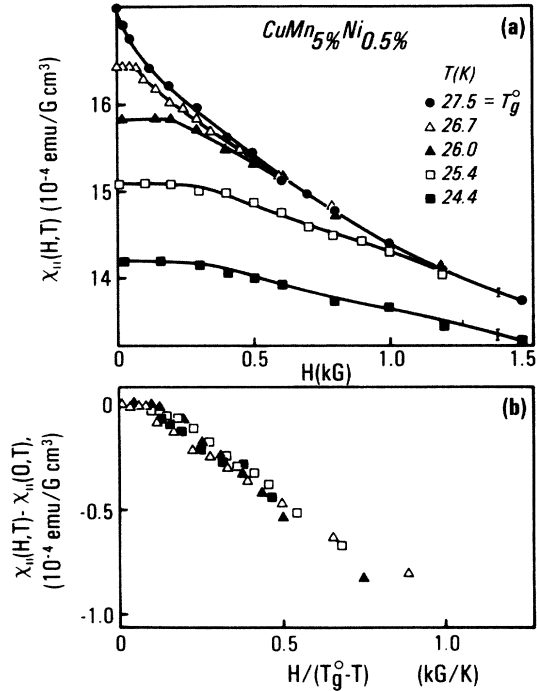


FIG. 7. (a) Values of $\chi_{\parallel}$ as a function of applied dc magnetic field for several values of temperature, all below $T_g^0$. Note this sample is for a Cu 5 at. % Mn–0.5 at. % Ni alloy, but is typical of that found for all the pure samples studied as well. The $\int_0^H \chi_{\parallel}dH$ is evaluated from the area under such curves as these. (b) The data of part (a) plotted as shown by the labeled axis. We find these data to be well represented by the scaling relations, as discussed in the text, with $\delta'=2$ and $\gamma'=1$.
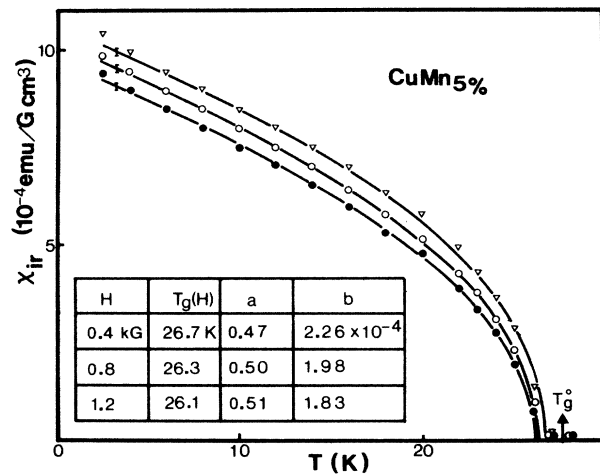


FIG. 8. The intrinsic magnetic remanent susceptibility, $\chi_{IR}$ as a function of temperature for several values of applied dc field. The triangles, open circles, and closed circles represent $H=0.4$, 0.8, and 1.2 kG, respectively. The procedure by which $\chi_{IR}$ is obtained from the $\chi_{\parallel}$, $\chi_{\perp}$, and $\chi_{dc}$ data is described in the text in detail. We note that $\chi_{IR}=b(1-T/T_g)^a$ with the values of $b$ and $a$ as given in the insert table. We regard $a$ as equal to $\frac{1}{2}$ to within the experimental errors, suggesting a very simple power-law dependence for $\chi_{IR}$.

enced by the initial oscillator. A digital voltmeter DVM (10) is used for monitoring the coil voltages. The residual pickup signal due to imperfect balancing of the coils is further canceled by adjusting the variable attenuator and phase shifter to produce a minimum output at temperatures well above $T_g$. The phase of the lock-in amplifier is set to detect the in-phase signal component at the same temperature. When using FET electronics for zero applied field, our sensitivity for the susceptibility was $3 \times 10^{-8}$ emu/G ac field. At an applied field of 1 kG the sensitivity was significantly reduced to $10^{-6}$ emu/G ac field. For measurements made utilizing the SQUID susceptometer, the sensitivity in zero field was $10^{-9}$ emu/G ac field and in an applied field of 5 kG, $10^{-7}$ emu/G ac field.

In Fig. 4 we present a scale diagram of the coil and sample arrangement. The sample (6) was moved back and forth between the two astatically wound coils (1) by a string (2) that was actuated outside the helium Dewar. The primary coil (3) was coaxial with the pickup coils. The assembly was contained within a constant-temperature shield (7) made of fine copper wires and epoxy so as to eliminate eddy-current pickup. The temperature was sensed by resistive elements, and suitable heaters are placed on the shield and in the helium to allow setting and stabilizing the temperature between 1.5 and 77 K.

### III. EXPERIMENTAL RESULTS

In Fig. 5 we present data which illustrates the comparison of the quantities $X_{dc}$ (open symbols), $X_\perp$ (closed symbols), and $X_{rev} \cong (1/H) \int_0^H X_{||} dH$ (solid line) for a Cu—5-at. % Mn sample. The three sets of data are for an applied dc field of $H=0.4$, 0.8, and 1.2 kG, respectively. (These data points are connected by fine lines as a guide to the eye.) The integral of $X_{||}(H)$ is obtained numerically from the smoothed data such as that illustrated in Fig. 6(a) (for $T > T_g^0$), and analogous sets of data for $T < T_g$, and is represented by the heavy curves. As discussed in Sec. II we expect $X_{rev}$, the susceptibility formed from the integral of $X_{||}$, to equal $X_{dc} = X_\perp$ for all $T \geq T_g^0$, and we regard the agreement as shown in Fig. 5 as confirmation of this assignment. Below $T_g^0$, we attribute the deviation between $X_{dc}$ and $X_{rev}$ to the presence of remanence, and have defined the difference as $X_{IR}$. Below $T_g^0$ we attribute the deviation between $X_\perp$ and $X_{rev}$ to the presence of both remanence and anisotropy energy, and determine $K$ via their difference utilizing Eq. (2).

In Fig. 6(b) we have replotted the data of Fig. 6(a) in the manner indicated by the labeled axis, and one sees that they obey a scaling relation.[11] The values of $\delta$ and $\gamma$ so obtained are $3 \pm 0.8$ and $1.85 \pm 0.5$, respectively. In Fig. 7(a) we present representative data for $X_{||}$ for $T < T_g^0$, for a sample of Cu—5 at. % Mn—0.5 at. %Ni. In Fig. 7(b) these data of Fig. 7(a) are replotted in the manner indicated by the labeled axis. Here we take the scaling relations for the $x$ axis to be of the form $f[H^{\delta'/2}/(T_g^0-T)^{\gamma'}]$, whence we find that these data are well fit with $\delta'=2$ and $\gamma'=1$.

In Fig. 8 we present our values for $X_{IR}$ obtained from the difference between $X_{dc}$ and $X_{rev}$ as a function of tem-

perature for several values of the applied dc field. The solid lines are fitted to these data using the relation $X_{IR} = b[T_g(H)-T]^a$, and the corresponding values of $a$, $b$, and $T_g(H)$ are shown in the insert. We note that the values of $a$ are all equal to $\frac{1}{2}$. The experimental uncertainties are for $a \pm 0.05$, and for $b \pm 1 \times 10^{-5}$.

In Fig. 9 we present values of $K$ obtained via different procedures as a function of temperature. The open symbols represent values obtained via use of Eq. (2) as follows. At a given $T$ and $H$, $X_\perp$ is measured, and we evaluate $(1/H) \int_0^H X_{||} dH$ from a set of $X_{||}$ data such as in Figure 6(a). We also have measured $M_{dc}$ and thereby determine $M_{IR}$ via Eq. (1). Thus we have all the quantities needed to obtain $K$ in a finite $H$. The solid circles represent the results of another set of $X_\perp$ measurements made in zero $H$. Here we turn off the field, wait 30 min. (for $M_r$ to effectively stabilize) and then measure $X_\perp$. The value of $M_r$, being relatively insensitive to the exact time, is measured separately in a SQUID dc magnetometer. Under these conditions Eq. (2) reduces to:

$$X_\perp = X_{||} + M_r^2/K .    \tag{3}$$

We note that the limitation to this procedure at higher temperatures is the rapid decay rate of $M_r$, but that over the $T$ range for which data were available there is satisfactory agreement with the values of $K$ deduced in zero $H$ up to 1.2 kG.

The solid squares represent values of $K$ deduced from ESR data taken at 9 GHz following the procedure intro-
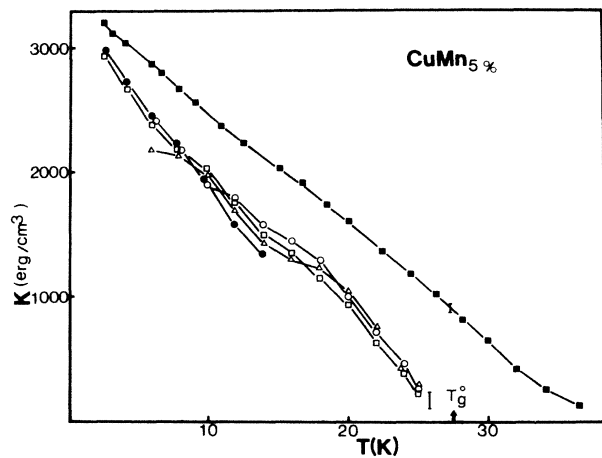


FIG. 9. The anisotropy energy constant as a function of temperature for a Cu—5 at. % Mn spin-glass sample. The solid circles are values deduced via Eq. (3) where the remanent magnetization is measured in zero field. The open symbols represent values of $K$ deduced via Eq. (2) and utilizing the $M_{IR}$ as explained in the text. (The open triangles, circles, and squares represent 0.4, 0.8, and 1.2 kG dc applied field, respectively.) We regard all these data to be within the experimental errors and well represented by the relation $K(T)=K(0)(1-T/T_g)$. The solid squares represent $K$ deduced by ESR measurements at 9.5 GHz as explained in the text. One sees that although both sets of data agree for $K(0)$, there is marked disagreement at temperatures near and above $T_g$.

duced by Schultz, et al.[3] In their analysis they have shown that $K = \delta H M(H_0)$, where $\delta H$ is the shift of the ESR resonance from the high-temperature ESR resonant field, $H_0$, and $M(H_0)$ is the total magnetization measured in the field $H_0$.

From the data of Fig. 9 we find we may represent the temperature dependence of $K(T)$ as

$$K(T) = K(0)(1 - T/T_g) \quad \text{(measured at 30 Hz)} \quad \text{(4a)}$$

and

$$K(T) = K(0)(1 - T/1.34T_g) \quad \text{(measured at 9 GHz)} \quad \text{(4b)}$$

In Fig. 10 we present the result of measurements wherein we checked as to whether the anisotropy energy of the system remains constant during an interval where the magnetic remanence is allowed to decay. The temperature was reduced from well above $T_g$ to the $T$ of interest. Then the field was turned off and $M_r$ was measured in the SQUID magnetometer as a function of time. [These data are the solid circles in Figs. 10(a) and 10(b).] In the ac apparatus we also measured $\chi_\perp$ for the identical field-time sequence. We also measured $\chi_{||}$, and from these sets of data determined the $K$ values corresponding to each measuring time via Eq. (3). As can be seen, $K$ does not decay in time to within the experimental uncertainty. (Note that since $K$ depends on $M_r^2$, this is a fairly good test procedure, despite the small percentage decay of $M_r$.)

In the course of making the measurements just described, we were able to test whether $\chi_{||}$ is a function of $M_r$. We found that at 10 K, over the time period during
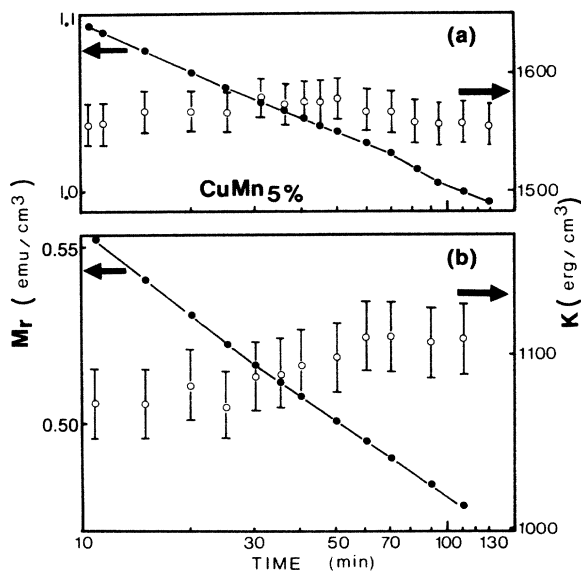


FIG. 10. (a) The time dependence of the magnetic remanence in zero field, $M_r$, (left axis) and the anisotropy energy constant, $K$, (right axis) at a fixed temperature of 10 K. (b) The time dependence of $M_r$ and $K$ similar to that in part (a), but for $T = 14$ K. We note that although there is an appreciable percentage decay in $M_r$, $K$ is determined to be time invariant to within the experimental uncertainty.

which $M_r$ decayed by 10%, $\chi_{||}$ was constant to within $\frac{1}{2}\%$. To further test this important point, we performed an auxiliary experiment. We cooled the sample in 20 kG (thereby making the largest $M_r$ that we could), and measured $\chi_{||}$ within several minutes following turning off the field. We then compared this value with $\chi_{||}$ measured at the same temperature, but cooled in zero field. Again, we found the same value of $\chi_{||}$ to within our experimental uncertainty ($\frac{1}{2}\%$).

We (and others) have explicitly assumed that $\chi_{||}$ itself is isotropic. While this symmetry is inherent to the model of triad dynamics[12,13] proposed for spin glasses, and notwithstanding the confirmation[14,15] of its key prediction of a longitudinal ESR mode, we felt it worthwhile to attempt some additional checks. In addition to taking data for h at 90° to H, we took data at an angle of 45°. We found that the 45° data, when suitably analyzed, yielded the same value of $K$ as that from $\chi_\perp$, thus confirming that the reversible part of susceptibility was the same at 45° and 90°.

## IV. DISCUSSION

We regard the temperature dependence of $\chi_{IR}$ and $K$ as presented in Figs. 8 and 9, respectively, as being the principal results of this work. Our commentary is as follows.

The excellent fit of the square-root relation for $\chi_{IR}$ is extremely suggestive due to its simplicity. We believe that similar data should be obtained at other frequencies and for additional materials to see if this relationship is a universal property of spin glasses. We do not know of a theoretical model that predicts this behavior for $\chi_{IR}$, but it would be important to ascertain if the simple dependence we have observed is contained within current theoretical formulations of the spin glass state.

From Fig. 9 it is clear that $K$ determined at 30 Hz extrapolates to zero very near $T_g^0$, which is agreement with torque measurements[16] but is in marked contrast to the temperature dependence of the anisotropy constant deduced from the ESR data. On the other hand, we note that if one extrapolates both curves to zero $T$ they are in close agreement. We again suggest that it would be very worthwhile to perform similar experiments to those reported here at intermediate frequencies in order to determine whether the temperature at which there is a peak in the zero field $\chi_{||}$, the temperature at which $K$ extrapolates to zero, and that at which $M_{IR}$ extrapolates to zero all have the same frequency dependence.[17] It is possible to conjecture that there really is an intrinsic remanence, relavent to the time scale of the measuring frequency, at temperatures well above the $T_g^0$ of 30 Hz. We might expect to find such an interpretation meaningful for frequencies up to $\approx 1$ GHz. Above 1 GHz, such as for the 9 GHz ESR data presented here, one must be more careful in the identification of $M_{IR}$, since the intrinsic spin relaxation times, $T_1$ and $T_2$ are both longer than the period of the applied ac field.

## V. CONCLUSIONS

From our detailed measurements of the temperature and dc field dependence of the dc magnetization, parallel

and perpendicular ac susceptibility, we have been able to obtain the following principal conclusions for measurements made at 30 Hz.

(i) $X_{||}$ is not a function of the magnetic remanence, even under conditions where $X_{||}$ is a function of the dc magnetic field.

(ii) Above the spin-glass transition temperature the $X_{dc}$ as measured directly, the quantity $(1/H)\int_0^H X_{||} dH$, and $X_{\perp}$ all agree within the experimental uncertainties verifying the self-consistency of the data, and the assumption of a purely reversible behavior.

(iii) Below the spin-glass transition temperature, we may determine an intrinsic magnetic remanence, $M_{IR}$, via time-independent measurement procedures, and this quantity obeys the simple relation $M_{IR} \propto (1 - T/T_g)^{1/2}$ over the entire temperature range of measurement.[18]

(iv) Utilizing the $M_{IR}$ we are able to deduce values for the anisotropy constant over a $T$ range to within 10% of $T_g$, and we find the simple relation $K = K(0)(1 - T/T_g)$. The value of $K$ at $T = 0$ agrees with that obtained by ESR methods, but is in marked contrast to the ESR relation at temperatures above $T_g$.

(v) The temperature field dependence of $X_{||}$ is well represented by scaling relations both above and below $T_g$, with the one below $T_g$ being particularly simple.

(vi) At those temperatures at which the remanent magnetization decays a readily measurable amount, the anisotropy energy remains unchanged.

In particular, we feel that the very simple relations found for the temperature dependence of $M_{IR}$ and $K$ indicate that they may be central to a characterization of the spin-glass state. Perhaps this simplicity also suggests that these relations should be able to be readily deduced from appropriate spin-glass models via physical reasoning.

We believe these data illustrate that very interesting properties of the spin-glass state may be studied via the simultaneous measurement of the three susceptibilities, $X_{dc}$, $X_{||}$, and $X_{\perp}$, as a function of magnetic field and temperature. We suggest that extension of this approach to a broad range of frequencies would provide fuller insight into the nature of the relaxation processes of the spin-glass state, which remains an important problem to be addressed at this time.

[1]C. A. M. Mulder, A. J. van Duyneveldt, and J. A. Mydosh, Phys. Rev. B **25**, 515 (1982); E. D. Dahlberg, M. Handiman, and J. Souletie, J. Phys. Lett. **39**, L-389 (1978).

[2]V. Cannella and J. A. Mydosh, Phys. Rev. B **6**, 4220 (1972).

[3]S. Schultz, E. M. Gullikson, D. R. Fredkin, and M. Tovar, Phys. Rev. Lett. **45**, 1508 (1980).

[4]A. J. van Duyneveldt and C. A. M. Mulder, Physica, **114B**, 82 (1982).

[5]D. J. Youm and S. Schultz, Phys. Rev. B **34**, 4771 (1986).

[6]F. Holtzberg, J. L. Tholence, and R. Tournier, *Amorphous Magnetism*, edited by R. A. Levy and R. Hasegawa (Plenum, New York, 1977), p. 155; R. Hoogerbeets, Wei-Li Luo, and R. Orbach, Phys. Rev. Lett. **55**, 111 (1985).

[7]S. Oseroff, M. Mesa, M. Tovar, and R. Arce, Phys. Rev. B **27**, 566 (1983).

[8]H. Alloul and F. Hippert, J. Magn. Magn. Mater. **31-34**, 1321 (1983).

[9]In principle the free energy may contain both uniaxial and unidirectional anisotropy terms. Since our measurements are constrainted to very small angular excursions, $K$ represents the sum of such possible terms.

[10]The SQUID susceptometer is manufactured by the Biomagnetic Technologies, Inc. Company.

[11]A. P. Malozemoff and Y. Imry, J. Magn. Magn. Mater. **31-34**, 1425 (1983).

[12]W. M. Saslow, Phys. Rev. Lett. **48**, 505 (1982).

[13]C. L. Henley, H. Sompolinsky, and B. I. Halperin, Phys. Rev. B **25**, 537 (1983).

[14]E. M. Gullikson, D. R. Fredkin, and S. Schultz, Phys. Rev. Lett. **50**, 537 (1983).

[15]E. M. Gullikson, R. Dalichaouch, and S. Schultz, Phys. Rev. B **32**, 507 (1985).

[16]N. de Courtenay, A. Fert, and I. A. Campbell, Phys. Rev. B **30**, 6791 (1984).

[17]In unpublished work, E. Guillikson and S. Schultz in a study of the temperature dependence of $K$ deduced from ESR experiments over a range from 2—18 GHz have shown a definite deviation from the simple linear behavior found at frequencies near 9 GHz. However, a quantitative analysis for temperature above $T_g$ is quite difficult at the lower frequency because of broader lines, less ESR shift, and possible sample-preparation complications.

[18]We note that within a few tenths of degree of $T_g^0$, quantities such as $X_{||}$ in zero field are very sensitive to the sample annealing and history. We did not attempt to study such a detailed behavior in this work.
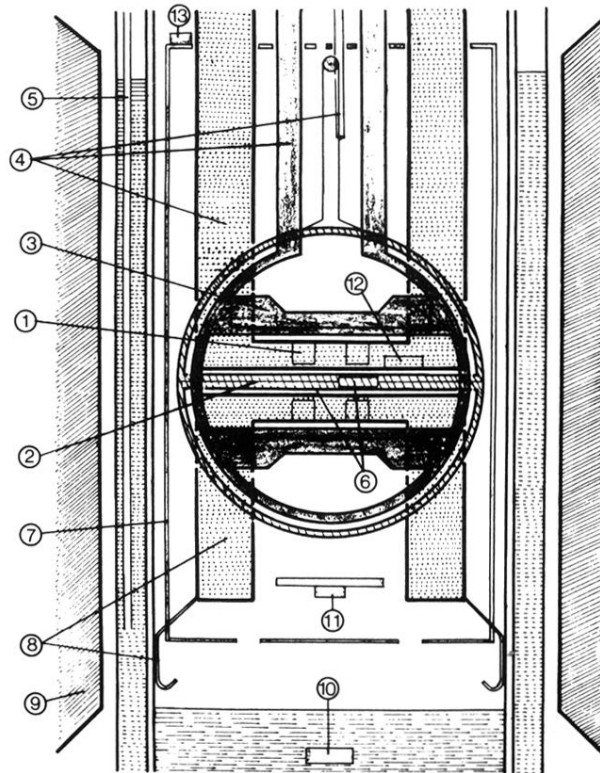
FIG. 4. Detailed scale drawings of the coils and sample arrangement. (1) the astatically wound pickup coils, (2) fine string used to push/pull the sample between the two coils of (1), (3) the primary ac coil, coaxial to (1), (4) various parts of the support system to hold coils firmly in helium Dewar, (5) a fine gas tube in liquid nitrogen jacket through which gas is blown to reduce bubbling, (6) sample holder containing rolled foil sample which slides in plastic tube, (7) temperature shield, (8) massive plastic holder with spring fingers to reduce vibration in helium Dewar, (9) external dc magnetic field, Varian rotatable magnet with 4-in. gap, (10) heater in liquid helium to produce cooling vapor, (11) heater on thermal shield to regulate temperature, (12) cryogenic thermometer, (13) additional heater to maintain shield at desired uniform temperature.